Binding of Surfactants onto Preadsorbed Layers of Bovine Serum Albumin at the Silica−Water Interface

J. R. Lu* and T. J. Su

Department of Chemistry, University of Surrey, Guildford GU2 5XH, U.K.

R. K. Thomas

Physical and Theoretical Chemistry Laboratory, South Parks Road, Oxford OX1 3QZ, U.K.

Received: July 22, 1998; In Final Form: September 25, 1998

The binding of nonionic and anionic surfactants from bulk solutions onto preadsorbed layers of bovine serum albumin (BSA) at the hydrophilic silicon oxide/water interface has been studied using specular neutron reflection. The distributions of surfactant, protein, and water at the solid/aqueous interface were separately determined by using deuterium labeling of the surfactant and water. The preadsorbed BSA layers were formed by equilibrating the hydrophilic oxide surface with a 0.15 g dm^{-3} BSA solution, which produced a densely packed uniform BSA layer of thickness 35 ± 3 Å. The possible association of nonionic surfactant pentaethylene glycol monododecyl ether (C_{12} E_5) with BSA at the interface was examined by following the change in neutron reflectivity before and after surfactant addition. That no measurable difference between these reflectivity profiles was observed suggests that the nonionic surfactant did not bind to the adsorbed BSA. The binding of sodium dodecyl sulfate (SDS) onto the BSA layer was studied over a wide SDS concentration range. Noticeable binding was detected at an SDS concentration of 1×10^{-4} M, and as the SDS concentration increases the thickness of the mixed layer also increases. At [SDS] $= 1 \times 10^{-3}$ M the reflectivity profile from the mixed layer became identical to that between the bare oxide/D_2O interface, suggesting that at this SDS concentration the mixture is completely removed from the interface. The surface excesses of BSA and SDS, and the structural distributions of BSA, SDS and water at each SDS concentration were obtained by simultaneously fitting a single structural model to the set of measured neutron reflectivity profiles. The results show that at low SDS concentrations the structural profiles of the interfacial components are well approximated as uniform layer distributions and as SDS concentration is increased the distributions become unsymmetrical. The binding of SDS results in an expansion of the preadsorbed BSA layer from 35 ± 3 Å in the absence of SDS to some 80 Å at 3×10^{-4} M, suggesting considerable structural deformation of the protein. The volume ratio of SDS to BSA in the mixed layer was found to be 0.45, in close agreement with the literature value for the binding of SDS onto denatured protein in the bulk, suggesting that the protein in the adsorbed complex is also denatured.

Introduction

The binding of surfactants to proteins at the solid/aqueous interface is of direct relevance to the removal of proteins deposited on many surfaces of practical interest, for example, contact lenses, surgical devices, food processing plants, and the ceramic membranes used in the purification of proteins. Protein adsorption often results in a heterogeneous layer which may decompose with adverse biological consequences.[1] The removal of adsorbed proteins is usually achieved by using surfactant formulations which may act by coadsorption into the protein layer.[2]

The key step in understanding the role played by surfactants is to determine the individual structural distributions of protein and surfactant. This is particularly important in the case of a globular protein since initial adsorption of the protein onto the solid substrate may result in some degree of deformation in the globular assembly and the binding of surfactants onto the adsorbed protein layer may cause further structural deformation, leading to the loss of the globular framework. The separate determination of the two distributions makes it possible not only to trace the fate of the globular protein but also to reveal the location of the surfactant binding. Few techniques are able to distinguish protein from surfactant in the mixed interfacial layer and as a result, few direct experiments have been made on the characterization of coadsorbed protein and surfactant at interfaces. There is therefore no sound understanding of the nature of the interaction of surfactants and proteins in these circumstances. The difficulties in making such measurements result from the lack of selectivity and resolution of existing experimental techniques. Several authors have shown that ellipsometry is capable of following the dynamic process of the binding of surfactant onto a protein layer adsorbed at the solid/water interface, but the technique cannot quantify the coadsorbed surfactant, nor can it identify the amount of protein remaining at the interface at a given surfactant concentration.[2−7] Radiolabeling, e.g., with I^{125}, can in principle identify the protein in the layer but it gives no structural information.[8]

Specular neutron reflection is a powerful technique for probing the structure of layers adsorbed at the solid/water interface. We have recently used neutron reflection to study

* Author to whom correspondence should be addressed.

10.1021/jp983126f CCC: $15.00
Published on Web 11/11/1998

the interaction of SDS and BSA at the hydrophilic silica/water interface. The structure and composition of surfactant, protein, and water in the complex adsorbed layer were determined separately by using deuterium labeling of the surfactant and water. The accurate determination of the structural dimensions helps to reveal any denaturation of the protein molecules before and after its interaction with the surfactant. This information can then be compared with the interaction of BSA with SDS in bulk solution, which has been well characterized by Tanford et al.[9] and Reynolds et al.[10] In bulk solution, the binding is predominantly driven by hydrophobic effects and is a competitive process involving the partitioning of surfactant between protein/surfactant aggregates and surfactant micelles.[9] The binding of surfactants onto globular proteins usually induces changes in conformation, leading to the breakdown of the globular structure of the protein.[9−14] It is therefore also of interest to examine how the globular structure of BSA is affected by SDS at the solid/water interface.

Experimental Section

Fatty acid-free BSA (molecular weight of BSA is 66 700 ± 400) was purchased from Sigma (Cat. No. A0281, Lot No. 10H9304) and was used as supplied. D_2O (99.9% D) was obtained from Fluorochem, and its surface tension was typically better than 71 mN m^{-1} at 298 K, indicating the absence of any surface-active impurity. H_2O was processed through an Elgastat ultrapure water system (UHQ), and its surface tension at 298 K was constant at 71.5 mN m^{-1}. The solution pH was controlled by using phosphate buffer at pH 5, keeping the total ionic strength fixed at 0.02 M. There were small differences in pH between H_2O and D_2O but this was controlled to within 0.3 pH units. The glassware and Teflon troughs for the reflection measurements were cleaned using alkaline detergent (Decon 90) followed by repeated washing in UHQ water. All the experiments were performed at 298 K.

Deuterated SDS was made by reacting deuterated dodecanol with chlorosulfonic acid in dry ethyl ether below 5 °C and the procedure concerning the synthesis and purification has been previously described.[15] The deuterated dodecanol used was made by reducing deuterated dodecanoic acid with $LiAlD_4$ (Aldrich, 98%+ D). The solid SDS sample was recrystallized from a water/ethanol mixture several times before a surface tension measurement was made to check the purity of the sample. The absence of a minimum in the surface tension plot at concentrations near the critical micelle concentration (CMC = 8.1×10^{-3} M) indicated a high purity of the deuterated sample. The extent of deuteration among the 25 hydrogen atoms in the dodecyl chain was found to be 96 ± 2% by NMR. Hydrogenated SDS was purchased from Polysciences (99%+) and was recrystallized several times before use. Its surface tension was found to be the same as that of the deuterated sample and the tension curves were also in good agreement with previous measurements.[16]

The large (111) face of the silicon block was polished using an Engis polishing machine. The block was lapped on a copper plate with 3 μm diamond polishing fluid and on a pad with 1 μm diamond followed by 0.1 μm alumina. The freshly polished surface was immersed in neutral Decon solution (5%) and ultrasonically cleaned for 30 min, and this was followed by a further 30 min of ultrasonic cleaning in water. The block was then rinsed and soaked in acid peroxide solution (600 mL 98% H_2SO_4 in 100 mL 25% H_2O_2) for 6 min at 120 °C.[17] The block was then thoroughly rinsed with UHQ water to remove acid, and exposed to UV/ozone for 30 min to remove any traces of organic impurities.[18] It was then left to soak in UHQ water for at least 24 h. This procedure was found to give surfaces with reproducible thickness and roughness of the oxide layer and which were completely wetted by water.

Neutron reflection experiments were performed on the white beam reflectometer CRISP at the Rutherford−Appleton Laboratory, ISIS, Didcot, U.K.[19] using neutron wavelengths from 1 to 6 Å. The sample cell was almost identical to that used by Fragneto et al.[20] with the aqueous solution contained in a Teflon trough clamped against a silicon block of dimensions $12.5 \times 5 \times 2.5$ cm^3. The collimated beam enters the end of the silicon block at a fixed angle, is reflected at a glancing angle from the solid/water interface, and exits from the opposite end of the silicon block. Each reflectivity profile was measured at three different glancing angles, 0.35°, 0.8°, and 1.8°, and the results combined. The beam intensity was calibrated by taking the intensity below the critical angle for total reflection at the silicon oxide/D_2O interface to be unity. A flat background determined by extrapolation to high values of momentum transfer, κ [$\kappa = (4\pi \sin \theta)/\lambda$ where λ is the wavelength and θ is the glancing angle of incidence], was subtracted. For all the measurements the reflectivity profiles were essentially flat at $\kappa > 0.2$ $Å^{-1}$, although the limiting signal at this point depends on the H_2O/D_2O ratio. The typical background for D_2O runs was 2×10^{-6}, and that for H_2O was 3.5×10^{-6} (measured in terms of the reflectivity).

Neutron Reflection

Neutron reflectivity $R(\kappa)$ is defined as the ratio of the reflected beam intensity to that of the incoming one and is primarily determined by the variation of scattering length density $\rho(z)$ along the surface normal direction:[21,22]

$$R(\kappa) \approx \frac{16\pi^2}{\kappa^2} |\hat{\rho}(\kappa)|^2 \tag{1}$$

where $\hat{\rho}(\kappa)$ is the one-dimensional Fourier transform of ρ (z):

$$\hat{\rho}(\kappa) = \int_{-\infty}^{\infty} \exp(-i\kappa z)\rho(z)\, dz \tag{2}$$

The scattering length density depends on the chemical composition through the following equation:

$$\rho = \sum n_i b_i \tag{3}$$

where n_i is the number density of element i and b_i is its scattering amplitude. The three equations given above formally demonstrate the relationship between neutron reflectivity and the structural profile across the interface.

The main strength of neutron reflection is the dependence of neutron reflectivity on the scattering length b_i as outlined above. Because different isotopes have different values of b_i, isotopic substitution can be used to change the reflectivity for a given chemical structure and this is helpful in determining composition at a mixed interface. For systems containing hydrogen atoms, isotopic substitution can be achieved by interchange of H and D. Although it is not easy to obtain protein samples with a high deuterium content, it is relatively easy to vary the isotopic labeling of surfactant molecules. Because the scattering lengths of D and H are of opposite sign the scattering length densities of surfactant and water can be varied over a wide range, which can be used to highlight an adsorbed protein layer in different ways. A simple example of the benefit of varying the isotopic labeling is as follows.

When a surfactant is bound to a preadsorbed protein layer at the solid/D_2O interface the mixed interfacial layer has three components: protein, surfactant, and water, and it is not easy to obtain the volume fraction distribution of each component across the interface. However, if the surfactant is deuterated and its scattering length density is adjusted to be close to that of D_2O, the surfactant is approximately invisible. In these circumstances the reflectivity will give the volume fraction of the protein directly. If a similar measurement is then made using the fully hydrogenated surfactant the reflectivity gives the combined volume fraction of protein and surfactant in the layer and hence the volume fraction of the surfactant can be obtained by subtraction.

The structural profile across a given interface is usually obtained by fitting a model to the measured reflectivity using the optical matrix formalism, in which an assumed structure of the interfacial layer is divided into a suitable number of uniform sublayers for which the reflected amplitudes are calculated before being combined to give the overall reflectivity.[23] The calculated reflectivity is then compared with the measured one, and the structural parameters subsequently modified in a least-squares iteration to obtain the optimum fit. The parameters used in the calculation are the thicknesses of the sublayers, τ_i, and their corresponding scattering length densities, ρ_i. Since the scattering length density of a given layer varies with isotopic composition, the fitting of a set of isotopic compositions to a single structural model greatly reduces the possibility of ambiguity in the interpretation, although it adds to the complexity of the fitting procedure. The choice of number of sublayers depends on the complexity of the system, but the general procedure is to use the minimum number that will fit the whole set of data. The volume fractions of each component in a mixed sublayer can be expressed as:

$$\rho = \phi_p\rho_p + \phi_s\rho_s + \phi_w\rho_w \tag{4}$$

where ρ is the total layer scattering length density, ρ_p, ρ_s, and ρ_w are the scattering length densities of BSA, SDS and water, and ϕ_p, ϕ_s, and ϕ_w are their respective volume fractions in the layer. Thus, $\phi_p + \phi_s + \phi_w = 1$. If deuterated SDS is adsorbed onto BSA from D_2O where ρ_s is adjusted to be equal to ρ_w, eq 4 can be written as

$$\rho = \phi_p\rho_p + (1 - \phi_p)\rho_w \tag{5}$$

The surface excess of the protein in each sublayer can be expressed as

$$\Gamma = \frac{\tau(1 - \phi_p)}{n'_w V_w N_a} \tag{6}$$

where τ is the thickness of the protein layer, n'_w is the number of water molecules associated with each protein molecule, V_w is the water molecular volume, and N_a is the Avogadro's constant. n'_w contains a contribution from the deuterated SDS and can be evaluated from the following equation:

$$n'_w = \frac{(1 - \phi_p)b_p}{\rho V_w - b_w(1 - \phi_p)} \tag{7}$$

where b_w and b_p are the scattering lengths for water and protein. Because ρ_p is known, ρ_s and ρ_w can be obtained by applying eq 4 to a reflectivity measurement at different contrast. Similarly, the exact value for the number of water molecules associated with each protein molecule can also be obtained. The set of equations above applies to a single sublayer and total adsorbed amounts, etc. are obtained by summing over the sublayers used in the fitting procedure.

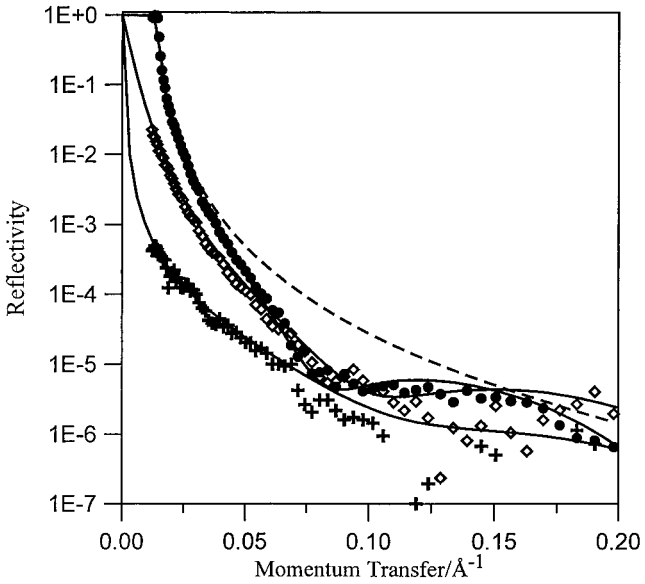

Figure 1. Neutron reflectivity profiles showing the adsorption of BSA at the silica/water interface from 0.15 g dm^{-3} phosphate-buffered BSA solution under D_2O (●) and CMSi (+) ($\rho = 2.07 \times 10^{-6}$ Å^{-2}) and H_2O (◇). The solution pH was 5.0, and the ionic strength was 0.02 M. The continuous lines were calculated for a BSA layer thickness of 35 ± 3 Å and a protein volume fraction of 0.45. The reflectivity from the bare silicon oxide/D_2O interface is also shown as a dashed line for comparison.

Results and Discussion

(A) Structure of the Oxide Layer. Before adsorption of any protein or surfactant is made the thickness and composition of the oxide layer present on the freshly polished silicon (111) surface has to be determined. This is because the structure of the oxide layer varies slightly from block to block and its exact composition contributes to the reflectivity, hence having a small effect on the determination of the amount of protein adsorbed. The structural characteristics of the oxide layer are easily determined by measuring its neutron reflectivity profile with the block in contact with water using the sample cell described in the Experimental Section. The water helps to highlight the features of the oxide layer, especially when it is defective. Measurements were made at two different water contrasts, D_2O and water whose scattering length density is matched to silicon (CMSi, $\rho = 2.07 \times 10^{-6}$ Å^{-2}). The resultant reflectivity profiles for the particular Si block used here have already been presented and analyzed [see ref 15, (Figure 1)]. The reflectivity is weak for CMSi because at this contrast the signal is only from the oxide layer. Water may penetrate any defects in the oxide layer and this would result in the total scattering length density for the oxide layer being lower than that of pure silica (3.41×10^{-6} Å^{-2}) in CMSi, but in D_2O the total scattering length density of the oxide layer would be higher than that of pure silica. However, all the reflectivity profiles were fitted using a thickness of 8 ± 3 Å and $\rho = 3.41 \times 10^{-6}$ Å^{-2} for the oxide layer, suggesting that, for the block used, there is no penetration of water into the layer, since the scattering length density of the layer is exactly as expected for amorphous oxide. No roughness was required in the fitting of the reflectivity, suggesting that the oxide surface is quite smooth.

(B) Structure of the Adsorbed BSA Layer. In the present series of experiments the BSA layer was adsorbed at a single bulk BSA concentration of 0.15 g dm^{-3}. The structural composition of the BSA layer was determined by varying the contrast of water. Figure 1 shows the measured reflectivity profiles in D_2O, CMSi (D_2O:$H_2O \approx$ 2:3) and H_2O. The simultaneous fitting of the three reflectivity profiles gives the thickness of the BSA layer as 35± 3 Å with a surface excess of 2.5 ± 0.3 mg m^{-2}, in good agreement with our previous results.[24] The excellent fits of the calculated curves to the data suggest that the uniform layer model is a good approximation for the protein layer distribution. We have shown in our previous work that over the BSA concentration between 5×10^{-3} and 0.3 g dm^{-3} BSA adsorption onto the hydrophilic silica gives a uniform layer between 30 and 36 Å thick. That the surface excess increases very little with bulk concentration suggests that BSA has a high surface affinity for the solid substrate. Since BSA is approximately cylindrical and its globular dimensions are $41 \times 41 \times 141$ $Å^3$, the measured layer thickness of 35 Å at 0.15 g dm^{-3} suggests that the molecules adsorbed sideways-on, that is, the long axis of the BSA molecule is parallel to the solid/water interface. That the actual layer thickness is less than the short axis of the molecule suggests that there is some degree of deformation upon surface adsorption. However, there is no sign of denaturation, since any breakdown of the globular framework resulting from denaturation would normally give rise to a diffuse layer, which would then be impossible to represent as a single smooth uniform layer. For example, adsorption of the globular lysozyme onto the hydrophobic surface formed by chemically grafting a monolayer of octadecyl trichlorosilane (OTS) onto silica leads to a more fragmented distribution of protein similar to the adsorbed layers formed by synthetic surface-active polymers.[25] The present results therefore indicate that, although there is some minor deformation, the globular framework basically remains intact upon adsorption.

Many authors have reported that protein adsorption onto the solid/solution interface is time dependent. For example, in several ellipsometric experiments the ellipsometric signal changes significantly over the first 30 min.[2−5] We have monitored the reflected neutron signal over similar time periods and found no observable changes. The first neutron reflection measurement was made within the first 10 min of contacting the BSA solution with the solid surface and therefore indicates that there are no changes in either the amount adsorbed or the structure of the BSA after the first 10 min. The changes in the ellipsometric signal cannot therefore be associated with changing amounts of protein at the surface, as has generally been assumed. We do not have an explanation for this discrepancy but, as we have indicated previously, the ellipsometric signal may be sensitive to the presence of counterions and to their type and these may continue to change after the protein adsorption is essentially complete. In contrast, neutron reflection is only directly sensitive to the protein itself.

Protein adsorption may be sensitive to variations in the hydrophilicity of the oxide surface and, since this could conceivably change during the course of the experiment, we also monitored the reflectivity profiles of BSA adsorbed at the silica/D_2O interface during the course of the experiment. After each SDS binding experiment the solid surface was cleaned by rinsing with SDS solution at its cmc and this was followed by copious rinsing with UHQ water and a final rinsing with D_2O. The standard 0.15 g dm^{-3} solution in D_2O was then introduced into the sample cell. No observable difference was found for BSA adsorption at different stages of the experiment, showing that the BSA/D_2O interface remained unchanged throughout the experiment and that the affinity of BSA for the surface did not change.

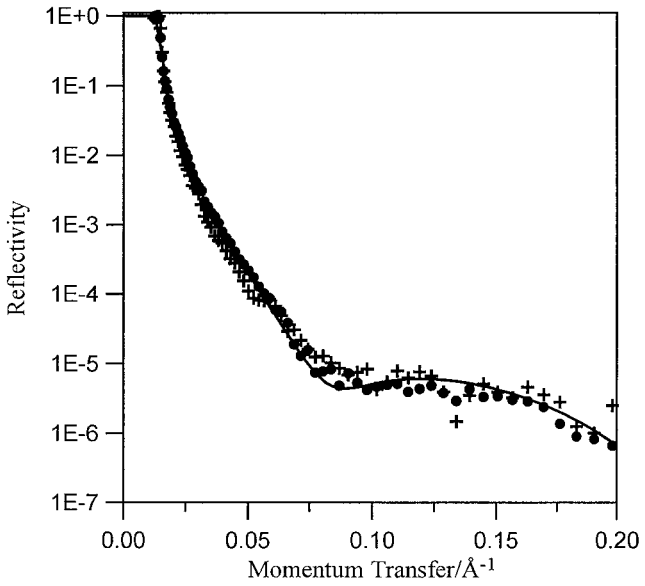

Figure 2. Neutron reflectivity profiles showing the possible coadsorption of C_{12} E_5 (+) onto the preadsorbed BSA at the silica/D_2O interface. The measured reflectivity from 0.15 g dm^{-3} BSA before the surfactant (●) was introduced was also shown for comparison. The solution pH was 5, and the ionic strength was 0.02 M. No observable difference in the two reflectivity profiles within the experimental error suggests that there is very little binding of C_{12} E_5 onto the preadsorbed BSA layer. The continuous line was calculated for a protein layer thickness of 35 ± 3 Å and $\rho = 5 \times 10^{-6}$ $Å^{-2}$.

(C) Binding of Nonionic Surfactant. The interaction of nonionic surfactants with globular proteins in bulk solution has been extensively studied. Initially it was thought that nonionic surfactants such as *p*-isooctyl-phenol ethoxylates do not bind to protein and therefore have no significant effect on the structural conformation of protein molecules. Nonionic surfactants were, in fact, regarded as the most mild and suitable surface-active materials for preparing lipid-free membrane proteins in their native conformation.[27] However, it was also found that nonyl-phenol ethoxylates could cause the loss of biological activities in some globular proteins, e.g., cytochrome oxidase, glucose-6-phosphatase, and adenylate cyclase.[28] Tanford et al.[9,26] later showed that nonionic surfactants interact with globular proteins and that their binding to native BSA was specific to the hydrophobic domains, in contrast to the cooperative association characteristic of anionic surfactants, as described below. The selective binding of nonionic surfactants usually results in the association of a small molar fraction of surfactant to protein. This may be large enough to have biological consequences without necessarily leading to denaturation. Using small-angle X-ray scattering Pradipasena et al.[29] have recently shown that the interaction between nonionic surfactants and proteins can cause the structural deformation of globular proteins without the breakdown of the globular framework.

Nonionic surfactant pentaethylene glycol monododecyl ether (C_{12} E_5) was used in this work and the possible binding of C_{12} E_5 with the BSA layer was monitored by following the change in neutron reflectivity. Figure 2 compares the reflectivity profiles in D_2O before and after surfactant addition. That there is no observable difference within experimental error suggests that, even if there is any interaction between surfactant and protein, the structural conformation of the adsorbed layer is little

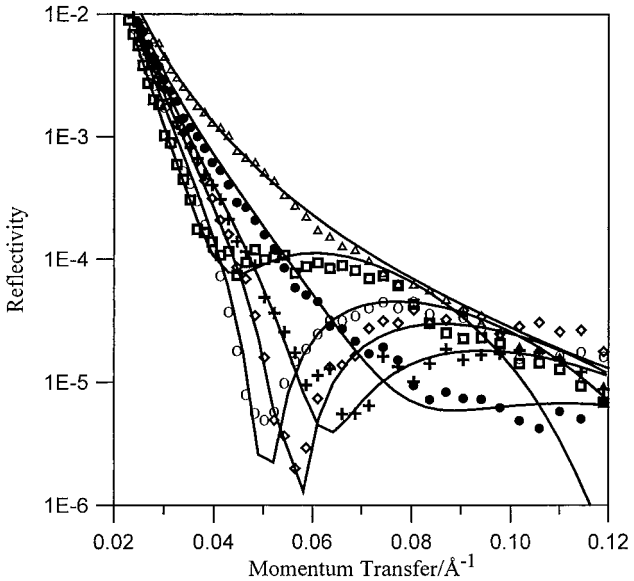

Figure 3. Neutron reflectivity profiles showing the binding of hydrogenated SDS onto the preadsorbed BSA layer in D_2O at the bulk SDS concentration of 0 M (●), 2×10^{-5} M (+), 1×10^{-4} M (◇), 2×10^{-4} M (○), 3×10^{-4} M (□), and 1×10^{-3} M (△). The continuous lines were calculated using the corresponding layer thickness of 35 ± 3 Å, 44 ± 3 Å, 50 ± 3 Å, 58 ± 5 Å, 80 ± 10, and 0 Å. That the reflectivity at 1×10^{-3} M SDS is the same as that from the bare oxide/D_2O interface (indicated as the continuous line through (△) suggests that the SDS/BSA complex has been completely removed from the interface.

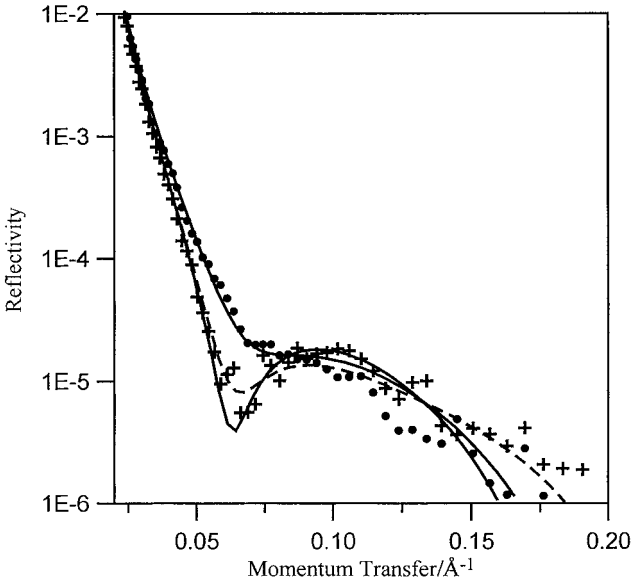

Figure 4. Neutron reflectivity profiles showing the effect of binding of *h*-SDS (+) and *d*-SDS (●) to the preadsorbed BSA layer in D_2O at 2×10^{-5} M SDS. The continuous lines were calculated using a uniform layer model with the layer thickness of 44 ± 3 Å and values of ρ corresponding to volume fractions of 0.38 for BSA, 0.09 for SDS, and 0.53 for water. The dashed line through the *h*-SDS/BSA profile was calculated using a two-layer model with an inner layer of 15 Å lean in SDS and an outer layer of 30 Å rich in SDS. The corresponding SDS volume fraction was 0.05 and 0.12, and the total SDS surface excess was within error the same as the value from the uniform layer model.

affected. This result does not contradict what was observed for this system in bulk solution[26] since if there are very few nonionic surfactant molecules bound to each protein molecule the effect on the reflectivity can be expected to be negligible. It may be that the presence of a phenyl group in the hydrophobic portion of the surfactant is essential for binding with the protein. The binding of alkylethoxylates onto preadsorbed lysozyme at the silicon oxide/water interface has been studied by Aenebrant and Wahlgren using ellipsometry. These authors observed a small increase in the total adsorbed amount after C_{12} E_5 was introduced into the solution, suggesting that there is weak association between the nonionic surfactant and protein at the interface, but, since the change in signal was small, they concluded that this type of nonionic surfactant does not interact strongly with the preadsorbed lysozyme. This result is consistent with the observation from our neutron measurements. Finally, it should be noted that, since these nonionic surfactants adsorb onto the hydrophilic silicon oxide/water interface to form a surfactant bilayer with their alkyl chains sandwiched in the middle,[30] no adsorption of surfactant following preadsorption of BSA indicates that the oxide surface was completely covered by BSA.

(D) Binding of Anionic Surfactant. The binding of sodium dodecyl sulfate (SDS) with proteins in bulk solution has been well characterized.[9,10] Figure 3 shows the effect of SDS concentration on the neutron reflectivity measured in D_2O. The reflectivity profile from the pure BSA/D_2O is shown for comparison. A noticeable change in the reflectivity occurs at 2×10^{-5} M, indicating that around this concentration the presence of SDS has caused structural changes to the protein layer. It can be seen from Figure 3 that an increase in the SDS concentration produces sharp minima in the reflectivity curves and that the position of these minima shifts toward low κ, indicating that the interfacial layer is increasingly thickened as more SDS is incorporated into the layer. It is probable that the thickening of the layer is related to the association of SDS with the protein, but how the structural conformation of BSA is affected cannot be deduced from measurements at this contrast. Equally, it is not clear how SDS molecules are distributed at the interface since the increase in the layer thickness may result from the adsorption of SDS molecules on the outer surface of the BSA layer. A further possibility is that as the SDS concentration increases the preadsorbed BSA is partially removed from the interface, as has been suggested by ellipsometry.[2] The complex structure of the mixed layer can be resolved by using deuterium labeling, in turn, of surfactant and water, as will be described below. Figure 3 also shows that, when the SDS concentration increases above 1×10^{-3} M, the neutron reflectivity from the mixed interfacial layer is identical to the one from the bare silicon oxide/D_2O interface, suggesting that all the organic materials have been removed from the interface. It should be noted that, at pH 5, SDS does not adsorb onto the bare silicon oxide/water interface. This is because the oxide surface at this pH carries weak negative charges[31] and SDS is also negatively charged.

The presence of SDS can be masked by using 96% deuterated SDS (*d*-SDS) whose scattering length density is identical to that of D_2O. When the measurement is made in D_2O together with SDS deuterated at this level, the only contribution to the reflectivity is approximately from the protein. Figure 4 compares the measured reflectivity profile using d-SDS at 2×10^{-5} M with the profile using hydrogenated SDS (*h*-SDS) at the same concentration. The difference between the pure BSA/D_2O profile (not shown in Figure 4 for clarity) and that of BSA/*d*-SDS/D_2O directly reflects the change in the distribution of the BSA layer caused by the presence of SDS in the layer since the *d*-SDS is effectively invisible under these conditions. Similarly, the difference between the profiles from BSA/*h*-SDS/D_2O and BSA/*d*-SDS/D_2O results only from the bound SDS in the layer. Thus, even without any quantitative analysis of the

TABLE 1: Scattering Length Densities of BSA in Different Water Contrasts at pH 5[a]

contrast	$\rho \times 10^6/\text{Å}^{-2}$
D_2O	3.33
CMSi	2.40
H_2O	1.82

[a] The total molecular volume was taken to be 79 111 Å^3.[38] The degree of ionization of different amino acid groups was taken from ref 39. The scattering length density of *d*-SDS was found to be 6.36×10^{-6} Å^{-2}, and that for *h*-SDS was 4×10^{-7} Å^{-2}.

data, it is already clear that SDS is substantially associated with the BSA layer and that the protein distribution itself changes in the presence of SDS.

Quantitative information regarding the distributions of the three components across the interface can be obtained through model fitting. The amount of protein adsorbed (surface excess) was obtained by fitting a uniform layer model to the reflectivity profiles using the optical matrix formalism already outlined. The continuous line through the measured reflectivity profile of BSA/*d*-SDS/D_2O in Figure 4 was calculated for a uniform layer of protein with a layer thickness of 44 ± 3 Å. The volume fraction of the adsorbed protein in the surface layer can be calculated from eqs 4 and 5 where $\rho_s = \rho_w$. Similarly, the surface excess of the adsorbed protein can be calculated using eqs 6 and 7 with the values of the physical constants for pure protein and surfactants at the appropriate isotopic composition given in Table 1. The good fit of a single uniform layer to the measured reflectivity profile under this contrast shows that although the protein layer has been expanded at this SDS concentration its distribution can be well represented by a uniform layer model. The continuous line through the measured reflectivity profile of BSA/*h*-SDS/D_2O is the uniform layer fit with the same total layer thickness. It can be seen from Figure 4 that the fitted curve follows the measured reflectivity profile well up to 0.13 Å^{-1}, beyond which deviation starts to occur. Since there is a large contribution from the hydrogenated SDS at this contrast, the result suggests that to a good approximation the mixed layer can also be represented by a uniform layer model. This indicates that the distribution of SDS molecules throughout the mixed layer is reasonably uniform. The volume fraction of SDS and its surface excess in the mixed surface layer can again be calculated using eqs 4 and 5.

The binding of SDS to proteins may be time dependent, and in several previous studies of the binding of SDS to different proteins in bulk solutions the mixed solutions were normally left for several hours to allow equilibrium to be reached before measurements were made.[32] We have examined the reproducibility and possible time effects by measuring the binding of *h*-SDS onto the preadsorbed BSA layer in two independent measurements. In the first measurement the BSA solution was in contact with the freshly cleaned oxide surface for just 5 min, the solution was then drained, and then buffered *h*-SDS solution added. The neutron reflectivity measurement of this sample was made within a period of 30 min. In the second measurement, the BSA solution was left in contact with the oxide layer for over a half hour before the BSA solution was drained and the preadsorbed BSA layer put in contact with *h*-SDS solution. The subsequent neutron measurements were made over a period of 2 h. No time effect in the BSA adsorption and the subsequent SDS binding was observed.

The effect of SDS concentration on the structural distribution of the BSA layer can be seen by comparing the reflectivity profiles in the presence of *d*-SDS, and this comparison is made in Figure 5. As already indicated, at this contrast the signal

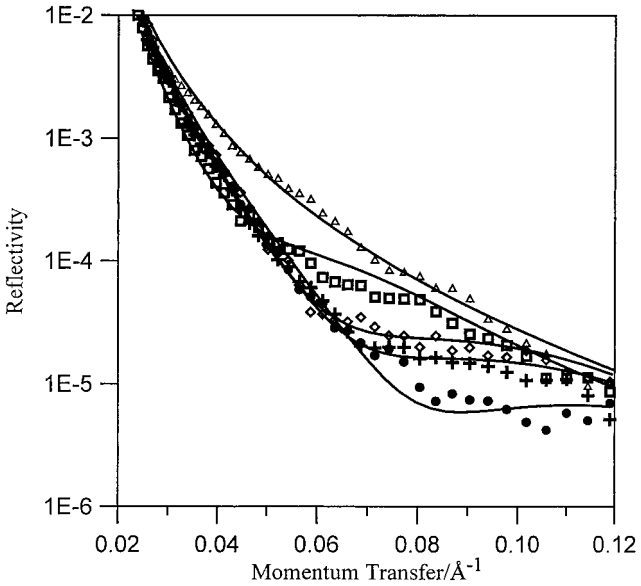

Figure 5. Neutron reflectivity profiles showing the binding of deuterated SDS onto the preadsorbed BSA layer in D_2O at the bulk SDS concentration of 0 M (●), 2×10^{-5} M (+), 1×10^{-4} M (◇), 3×10^{-4} M (□), and 1×10^{-3} M (△). The continuous lines were calculated using the corresponding layer thickness of 35 ± 3 Å, 44 ± 3 Å, 50 ± 3 Å, 80 ± 10, and 0 Å. That the reflectivity at 1×10^{-3} M SDS is the same as that from the bare oxide/D_2O interface (△) suggests that the SDS/BSA complex has been completely removed from the interface.

gives direct information about the distribution of the protein layer in the presence of SDS while SDS itself is contrast matched out. It can be seen from Figure 5 that all the reflectivity profiles contain minima and the position of the minimum is shifted toward low κ with the increase of SDS concentration, suggesting that the protein layer is gradually expanded. The fits based on the uniform layer distribution produce a thickness of 50 Å at 1×10^{-4} M and this further expands to 70 Å at 3×10^{-4} M, which is twice as thick as the pure protein layer. Furthermore, as the concentration of *d*-SDS increases above 1×10^{-3} M the reflectivity returns to that for the bare silica/D_2O interface, a trend entirely consistent with that observed with *h*-SDS.

As the SDS concentration increases, the uniform layer model is found to be a less appropriate model for the distributions of protein and protein/SDS mixtures at the interface. The deviations mainly occur at $\kappa > 0.15$ Å^{-1}, and the data over this part of κ are not shown in Figures 3 and 5 for clarity. In fact, even at 2×10^{-5} M the uniform layer model does not fit the measured reflectivity profile for BSA/*h*-SDS/D_2O well over the high κ region (see Figure 4). The deviation is caused by the distribution of SDS because, at this concentration, the uniform layer model gives a good fit to the BSA/*d*-SDS/D_2O. The data were therefore fitted with a two-layer model with a 15 Å inner layer somewhat lean in SDS and a 30 Å outer layer rich in SDS. The dashed line in Figure 4 shows the best two-layer fit with a scattering length density for the inner layer of 5×10^{-6} Å^{-2} and for the outer layer of 4.4×10^{-6} Å^{-2}. The two-layer model significantly improves the fit at high κ. Since the distribution of BSA has already been established, the volume fraction of SDS in each layer can be calculated from eqs 4 and 5 to be about 0.05 for the inner layer and 0.12 for the outer layer. The resultant total surface excess is close to the value estimated from the single uniform layer model, which further confirms our previous observation that the uniform layer model offers a good estimate for the surface excess despite its poor fit to the shape

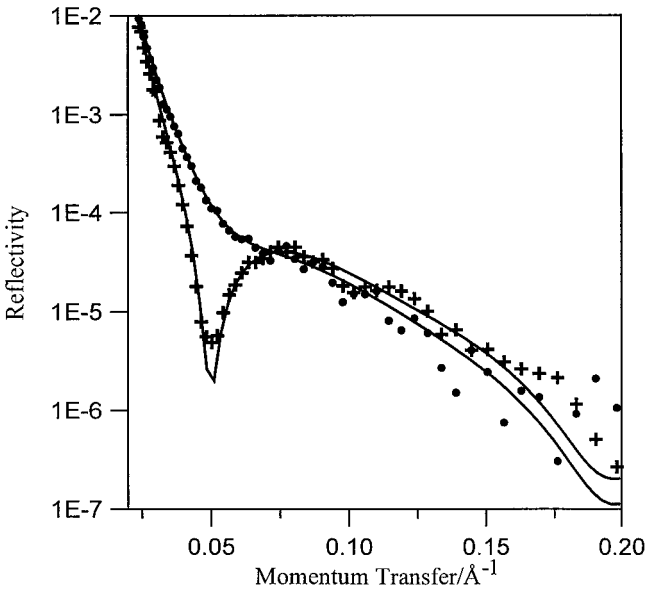

Figure 6. Neutron reflectivity profiles showing the effect of binding of *h*-SDS (+) and *d*-SDS (●) to the preadsorbed BSA layer in D_2O at 2×10^{-4} M SDS. The continuous lines were calculated using a three-layer model with an inner layer of 10 Å lean in the mixture, a middle layer of 36 Å rich in the mixture, and an outer layer of 25 Å lean in the mixture. The good fit of the three-layer model to the reflectivity profiles suggests that the mixed layer is unevenly distributed along the surface normal.

of the reflectivity profile.[21] The unsymmetrical distribution of SDS was only observed at the lowest SDS concentration and is probably caused by the partial retention of the globular structure and the consequent steric blocking of access of SDS molecules into the protein layer near the solid surface. At the higher SDS concentration the distribution of the BSA layer becomes less uniform. It is then diffficult to disentangle the structural distribution for the SDS, as will be seen in the following.

The disintegration of the adsorbed BSA at high SDS concentration can be followed to some extent by using more complex models to fit the reflectivity profiles measured with *d*-SDS. Figure 6 shows the improvement of the fits to the reflectivity profiles measured at 2×10^{-4} M in D_2O using a three-layer model. The three-layer model assumes that the protein/SDS mixture is depleted in the inner 10 Å close to the oxide surface, the middle layer of 36 Å contains the major fraction of the interfacial mixture, and the outer layer of 25 Å contains a small fraction of protein and surfactant and possibly consists of the disrupted polar fragments of the protein. In fitting the BSA/*d*-SDS profile the values of ρ used were 5.6×10^{-6} Å^{-2} for the inner layer, 5.2×10^{-6} Å^{-2} for the middle layer, and 6.1×10^{-6} Å^{-2} for the outer layer. Similarly, the values of ρ used for fitting the BSA/*h*-SDS profile were 5.3×10^{-6} Å^{-2} for the inner layer, 4.0×10^{-6} Å^{-2} for the middle layer, and 5.7×10^{-6} Å^{-2} for the outer layer. The result clearly indicates that the interfacial mixture is distributed unevenly. As the protein distribution is broadened with added SDS the layer becomes generally more depleted before complete removal of the layer occurs when SDS increases above 1×10^{-3} M. At this stage it is difficult to calculate the exact composition within each of the sublayers because the disintegration of the globular framework may promote more segregated distributions of the protein fragments within the interfacial region, just as in the case of surface adsorption of di-and triblock synthetic polymers. It then becomes unreliable to assign the same average scattering length density of pure protein to the fragments within each sublayer. Taking the two limits of complete mixing and of complete segregation of all the polar and charged groups from the nonpolar groups would lead to errors in composition of the sublayers of up to 100%. Although it is therefore not worthwhile to attempt any subdivision in the distribution of the protein fragments within each layer, the structural analysis nevertheless shows clearly the denaturing of the globular protein structure with increasing bulk SDS concentration.

The structural parameters obtained from the measurements at different contrasts are summarized in Table 2. It is interesting to see that the surface excess of BSA remains constant until the SDS concentration reaches 5×10^{-4} M, suggesting that protein removal from the surface does not start until the mixed layer has been extensively disrupted. This must be the reason that BSA removal occurs at a critical surfactant concentration instead of gradually as observed for the lysozyme/SDS system by Wahlgren et al. using ellipsometry.[7] The volume fraction of protein within the layer decreases steadily with the increase of layer thickness and the extra expanded volume is filled by water and bound SDS molecules. There is no obvious trend in the change of SDS volume fraction because it is partly determined by the distribution of BSA in the layer. This feature can be better understood in terms of the volume ratio of the two components. Initially, the ratio reaches a limit of 0.45, suggesting that binding reaches a saturation point at 1×10^{-4} M. The binding of SDS to a variety of proteins in bulk solution has been studied by Reynolds and Tanford.[33] These authors examined the binding of SDS to several denatured proteins and found that the weight ratio of SDS to protein was almost constant at 0.4 below 8×10^{-4} M SDS and this increased to 1.4 as the SDS concentration was increased. They also found that the binding only depended on the monomer SDS concentration and had little to do with the identity or molecular weight of the proteins. Thus, on breakdown of the native structures by β-mercaptoethanol or by a combination of guanidine hydrochloride (GuHCl) and β-mercaptoethanol, proteins are reduced to mixed polypeptide chains in a random coil conformation and the binding is then only determined by the number of peptide groups available. Reynolds et al.[13,14] also studied the binding of SDS onto native BSA and found that at SDS concentrations around 1×10^{-4} M the weight ratio is below 0.1, which is much lower than that for denatured proteins. Thus, the ratio of the observed volume fraction of 0.45 for the complex at the solid/water interface is close to the ratio of 0.4 for the binding of SDS on to denatured BSA. This suggests that binding of SDS to BSA at the solid/water interface results in the complete breakdown of the globular assembly so that all the hydrophobic domains are able to bind SDS.

In fitting the reflectivity profiles at different contrasts, it has been assumed that all labile hydrogens within BSA have exchanged completely with bulk water within the time scale of the neutron experiment of a few hours. It is not obvious that this should be the case because BSA has hydrophobic domains which may not be accessible to water. The extent of exchange of the labile hydrogens in globular proteins with D_2O has been extensively investigated in the past and has been reviewed by Hvidt and Nielsen.[34] More recently, Dobson et al.[35] have extended this work with the aim of revealing the mechanisms relating to the folding and unfolding of protein molecules under different solution conditions. The accessibility of labile hydrogen atoms to the surrounding water has been widely used as a measure of the masking of portions of the polypeptide chain. Of the 1015 potentially labile hydrogen atoms per BSA molecule, about 750 exchange almost instantly at pH 7 and 0 °C. Some further 200 exchange over a period of a few minutes

TABLE 2: Structural Parameters Obtained from Uniform Layer Model Fitting[a]

[SDS]/ 10^{-3} M	0	0.02	0.1	0.2	0.3	0.5
τ/ Å	35 ± 3	44 ± 3	50 ± 3	58 ± 5	80 ± 10	70 ± 20
Γ/mg m^{-2}	2.5 ± 0.3	2.6 ± 0.3	2.5 ± 0.3	2.6 ± 0.3	2.6 ± 0.3	2 ± 0.6
ϕ_p	0.45	0.38	0.38	0.34	0.24	0.15
ϕ_s	0	0.09	0.17	0.15	0.11	0.06
ϕ_s/ϕ_p	0	0.24	0.45	0.44	0.46	0.4

[a] Complete removal was obtained at [SDS] $= 1 \times 10^{-3}$ M.

up to 2 h, but the remaining 50−100 appear not to exchange easily within a further 24 h. Thus, about 90% of the labile hydrogens are readily exchangeable. Hvidt and Nielson also found that pH and temperature substantially affect the exchange rate. The most difficult hydrogens to exchange are those on the amide groups in the peptide chain, of which BSA has 582. The barrier preventing the exchange is the hydrophobic encapsulation of any labile hydrogens inside the globular structure, but since some of the labile hydrogens in the peptide chain are on the outer surface of the globular structure they are easily exchanged. The fraction which is buried inside the hydrophobic domains is not expected to exchange within the time scale of the experiment. This incomplete exchange will introduce an error in the scattering length and a consequent error in the derived surface excess. The typical uncertainty of the neutron reflection experiment is 5% or less. If, at the time of adsorption, exchange is incomplete by more than about 5%, one would expect to obtain a small difference in the BSA surface excess in the presence and absence of SDS. This is because the binding of SDS opens up the protein assembly and, since the binding is of hydrophobic origin, the buried labile hydrogens would be more exposed to the surrounding water. That the surface excess does not change suggests that exchange within the preadsorbed BSA layer, where the protein retains its native structure, although slightly distorted, is already complete.

The structure of the SDS/BSA complex in bulk solution has been examined by various techniques.[14,36,37] The binding sites have been a matter of interest and the determination of these has been based on changes in ultraviolet absorption or in optical rotation. Binding of SDS onto BSA shifts several ultraviolet bands in the wavelength range 2000−3000 Å, indicating that tryptophan residues are at or near the strongest binding sites and that additional sites with slightly lower affinity are at or close to tyrosine residues. Results from viscosity studies by Reynolds and Tanford[14] were modeled in terms of rodlike aggregates, and the data suggested that as the level of SDS binding increases the long axis of the protein becomes more extended. This model was later supported by dynamic light scattering measurements by Tanner et al.[37] which showed a consistent increase of the hydrodynamic radius with increased SDS binding. The results of Tanner et al. also showed that when the binding weight ratio was below 1 the short axial radius of the prolate spheroid was 21 Å and the long axial radius was about 80 Å, as compared with the values of 21 and 70 Å for the two corresponding radii for native BSA in solution. Thus, SDS binding apparently elongates the rodlike native structure but does not alter its cross-sectional diameter. This picture is not obviously consistent with what is observed at the solid/water interface. If the SDS/BSA complex retains its structure at the solid/water interface, the thickness of the mixed layer should be the same as the preadsorbed BSA without bound SDS. That the layer thickness has increased substantially suggests that the structure of SDS/BSA is different from that in bulk solution. Thus, the presence of the solid interface must have induced further structural deformation. The high packing density within the mixed protein layer and the geometrical constraint of the wall probably force the layer to expand when the globular framework is broken.

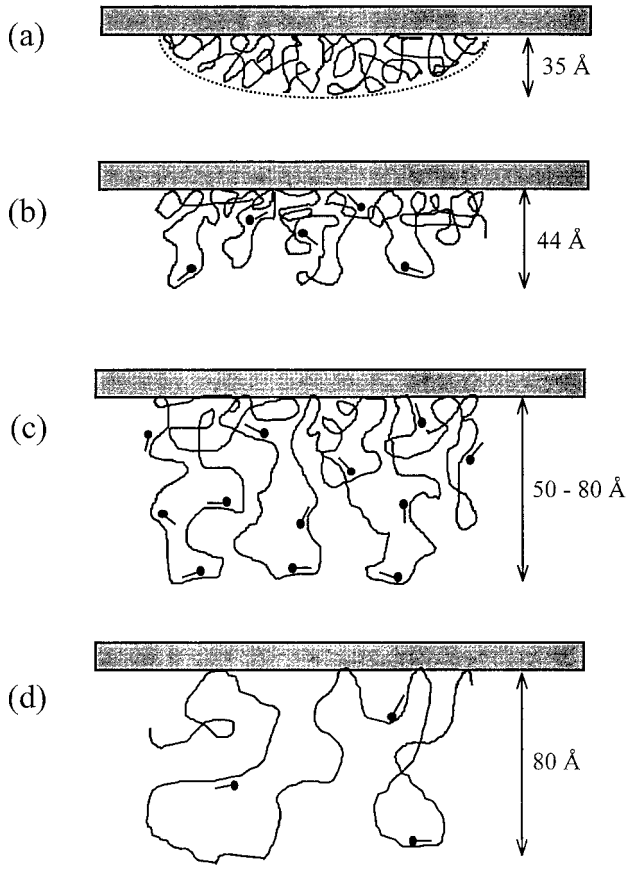

Figure 7. Schematic representation of the effect of SDS concentration on the disintegration of BSA globular structure: (a) representation of a BSA molecule adsorbed sideways-on, (b) binding of SDS onto BSA at a SDS concentration around 2×10^{-5} M, (c) [SDS] $= 2 \times 10^{-4}$ M, and (d) [SDS] $> 5 \times 10^{-4}$ M.

Conclusion

The breakdown of the adsorbed BSA layer under different SDS concentrations is schematically represented in Figure 7. The diagram is focused on featuring the expansion of the mixed layer with SDS concentration. Thus, structural details, e.g., the unsymmetrical SDS distributions at very low SDS concentration and the depletion of the complex in the region close to the solid substrate are not shown for simplicity. The adsorption of BSA onto the hydrophilic silicon oxide/water interface forms a sideways-on monolayer with retention of the globular structure. The adsorbed BSA layer is slightly thinner than the full diameter of the globular protein across its short axis, suggesting that there is some deformation after adsorption onto the solid substrate. When a small amount of SDS is added binding mainly occurs as a result of specific interaction and charge neutralization. As the SDS concentration approaches 1×10^{-5} M cooperative association between SDS and the adsorbed BSA occurs, leading

to an enhanced fraction of SDS bound to the adsorbed BSA molecules. Further increase in SDS concentration results in substantial expansion of the adsorbed protein and the consequent opening up of the hydrophobic domains within the BSA. When the SDS concentration is above 2×10^{-4} M the distribution of the mixed layer deviates from a uniform layer distribution, indicating that the disintegration of the protein framework is so extensive that the attachment of the layer to the solid substrate starts to be loosened. However, removal does not begin until the SDS concentration increases above 5×10^{-4} M. When the SDS concentration is above 1×10^{-3} M the mixture is completely removed from the solid/water interface.

Acknowledgment. We thank the Biotechnology and Biological Sciences Research Council for support. We also thank the staff at the ISIS Neutron Facilities for technical support.

References and Notes

(1) Andrade, J. D. In *Surface and Interfacial Aspects of Biomedical Polymers: Protein Adsorption*, Vol. 2; Andrade, J. D., Ed.; Plenum: New York, 1985.
(2) Arnebrant, T.; Wahlgren, M. C., In *Protein at Interfaces II*, ACS Symp. Ser. 602; Horbett, T. A., Brash, T. A., Eds.; American Chemical Society: Washington, DC, 1995.
(3) Elwing, H.; Askendal, A.; Lundstrom, I. *J. Colloid Interface Sci.* **1989**, *128*, 296.
(4) Wahlgren, M.; Arnebrant, T. *J. Colloid Interface Sci.* **1991**, *142*, 503.
(5) McGuire, J.; Wahlgren, M.; Arnebrant, T. *J. Colloid Interface Sci.* **1995**, *170*, 182.
(6) Ruardy, T. G.; Schakenraad, J. M.; Van der Mei, H. C.; Busscher, H. J. *Surf. Sci. Rep.* **1997**, *29*, 1.
(7) Wahlgren, M.; Arnebrant, T. *Langmuir* **1997**, *13*, 8.
(8) Rapola, R. J.; Horbett, T. A. *J. Colloid Interface Sci.* **1990**, *136*, 480.
(9) Tanford, C. *J. Mol. Biol*. **1972**, *67*, 59.
(10) Reynolds, J. A.; Herbert, S.; Polet, H.; Steinhardt, J. *Biochemistry* **1967**, *6*, 937.
(11) Steinhardt, J.; Scott, J. R.; Birdi, K. S. *Biochemistry* **1977**, *16*, 718.
(12) Nelson, C. *J. Biol. Chem.* **1971**, *246*, 3895.
(13) Reynolds, J. A.; Gallagher, J. P.; Steinhardt, J. *Biochemistry* **1970**, *9*, 1232.
(14) Reynolds, J. A.; Tanford, C. *J. Biol. Chem.* **1970**, *245*, 5161.
(15) Lu, J. R.; Su, T. J.; Thomas, R. K.; Penfold, J. *Langmuir* **1998**, *14*, 6261.
(16) Lu, J. R.; Su, T. J.; Morocco, A.; Thomas, R. K.; Penfold, J. *J. Colloid Interface Sci.* **1993**, *158*, 303.
(17) Brzoska, J. B.; Shahidzadeh, N.; Rondelez, F. *Nature* **1992**, *360*, 719.
(18) Vig, J. R. *J. Vac. Sci. Technol.* **1985**, *A3*, 1027.
(19) Penfold, J.; Richardson, R. M.; Zarbakhsh, A.; Webster, J. R. P.; Bucknall, D. G.; Rennie, A. R.; Jones, R. A. L.; Cosgrove, T.; Thomas, R. K.; Higgins, J. S.; Fletcher, P. D. I.; Dickinson, E.; Roser, S. J.; McLure, I. A.; Hillman, R. A.; Richards, R. W.; Staples, E. J.; Burgess, A. N.; Simister, E. A.; White, J. W. *J. Chem. Soc. Far. Trans.* **1997**, *93*, 3899.
(20) Fragneto, G.; Lu, J. R.; McDermott, D. C.; Thomas, R. K.; Rennie, A. R.; Gallagher, P. D.; Satija, S. K. *Langmuir* **1996**, *12*, 477.
(21) Lu, J. R.; Lee, E. M.; Thomas, R. K. *Acta Crystallogr.* **1996**, *A52*, 42.
(22) Crowley, T. L. *Physica A* **1993**, *195*, 354.
(23) Born, M., Wolf, E. *Principles of Optics*; Pergamon: Oxford, 1970.
(24) Su, T. J.; Lu, J. R.; Thomas, R. K.; Cui, Z. F.; Penfold, J. *J. Phys. Chem. B* **1998**, *102*, 8100.
(25) Su, T. J.; Lu, J. R.; Thirtle, P. N.; Thomas, R. K.; Rennie, A. R.; Cubitt, B. *J. Colloid Interface Sci.* **1998**, *206*, 212.
(26) Makino, S.; Reynolds, J. A.; Tanford, C. *J. Biol. Chem.* **1973**, *248*, 4926.
(27) Meyer, Y. P. *J. Biol. Chem.* **1971**, *246*, 1241.
(28) Rubin, M. S.; Tzagoloff, A. *J. Biol. Chem.* **1973**, *248*, 4268.
(29) Pradipasena, P.; Israeli, O.; Lu, M.; Chen, S. H.; Briganti, G.; Rha, C. In *Protein Structure Function Relationships in Foods*; Yada, R. Y., Jackman, R. L., Eds.; Blackie: 1994.
(30) McDermott, D. C.; Lu, J. R.; Lee, E. M.; Thomas, R. K.; Rennie, A. R. *Langmuir* **1992**, *8*, 1204.
(31) Iler, R. K. *The Chemistry of Silica*; Wiley: New York, 1979.
(32) Mascher, E.; Lundahl, P., J. *Chromatography* **1989**, *476*, 147.
(33) Reynolds, J. A.; Tanford, C. *Proc. Natl. Acad. Sci. U.S.A.* **1970**, *66*, 1002.
(34) Hvidt, A.; Nielsen, S. O. *Adv. Protein Chem.* **1966**, *21*, 287.
(35) Radford, S.; Buck, M.; Topping, K. D.; Dobson, C. M.; Evans, P. *Proteins* **1992**, *14*, 237.
(36) Mattice, W.; Riser, J. M.; Clark, D. S. *Biochemistry* **1976**, *15*, 4264.
(37) Tanner, R. E.; Herpigny, B.; Chen, S. H.; Rha, C. K. *J. Chem. Phys.* **1982**, *76*, 3866.
(38) Van Krevelen, D. W. *Properties of Polymers* (3rd ed); Elsevier: New York, 1990.
(39) Stryer, L. *Biochemistry* (3rd ed.); W. H. Freeman and Company: New York, 1988.